Friction **12**(1): 164–173 (2024)
https://doi.org/10.1007/s40544-023-0762-6
ISSN 2223-7690
CN 10-1237/TH
RESEARCH ARTICLE

Liquid superlubricity of lubricants containing hydroxyl groups and their aqueous solution under rolling/sliding conditions

Tomáš POLÁČEK*, Petr ŠPERKA, Ivan KŘUPKA
Faculty of Mechanical Engineering, Brno University of Technology, Brno 61669, Czech Republic
Received: 08 November 2022 / Revised: 14 January 2023 / Accepted: 21 March 2023

Abstract: Macroscale rolling/sliding conditions are in the superlubricity, a little-studied topic so far. The purpose of this paper is to examine the formation of elastohydrodynamic lubrication (EHL) films by water-based lubricants (glycerol and polyethylene glycol (PEG)), providing superlubricous friction. Experiments were carried out on an optical ball-on-disc tribometer under rolling/sliding conditions. The film thickness was measured by the thin film colorimetric interferometry, and the viscosity of liquids was measured by rotational and high-pressure falling body viscometers. The results show that tribochemical reactions are not the mandatory reason for friction to reach the superlubricity level when using the water-based lubricants. The studied liquids themselves are almost Newtonian. With the addition of water, the signs of shear thinning behavior disappear even more. Suitable conditions for this type of lubricant can be predicted using the known Hamrock–Dowson equations. An anomaly in the thickness of the lubricants was observed as an abrupt change at certain conditions. The more PEG there is in the lubricant, the higher the thickness at the beginning of the jump.

Keywords: macroscale superlubricity; super low traction; water-based lubricants; elastohydrodynamic lubrication (EHL); film thickness

1 Introduction

In the recent decades, a considerable effort has been put into understanding conditions and mechanisms of contact operation at very low friction, i.e., the coefficient of friction (CoF) below 0.01 called superlubricity [1]. The friction level corresponds to the resistance of needle bearings lubricated by engine oils such as 5W-30 [2, 3]. Superlubricity is divided into solid and liquid, where the former is sometimes called structural superlubricity [4]. It includes diamond-like carbon (DLC), carbon nitride (CN_x) coatings, molybdenum disulfide (MoS_2), graphite, fullerene, and other carbon nanoparticles [1, 4, 5]. These materials generally require special conditions such as an ultra-high vacuum, low or high temperature, or just low load. Researchers have focused on pure sliding in micro- or nanocontacts, and much fewer studies dealt with rolling [6] or sliding in macrocontacts [7].

The liquid superlubricity splits into water-based and oil-based [5]. Furthermore, it can be categorized according to function materials, e.g., water, polymer brushes, acid-based aqueous lubricants, room-temperature ionic liquid (RTIL), oil-based lubricants, and nanomaterial-based lubricants [8]. Oil-based lubricants have a larger pressure–viscosity coefficient (α^*) as well as ambient-condition viscosity compared to water-based lubricants. Li et al. [9] calculated a superlubricity region depending on an average pressure and the pressure–viscosity coefficient. They was stated that if the viscosity was strongly dependent on the pressure, the applied load has to be much smaller to achieve the superlubricity. Therefore, the oil-based superlubricity is rarely observed in contrast to glycerol, polyglycols, and its solution.

The reduction of friction by water, acid-based,

*Corresponding author: Tomáš POLÁČEK, E-mail: Tomas.Polacek2@vut.cz

and polymers lubricants is often explained as a tribochemically induced reaction between a contact tribopair and a lubricant [10–16]. Tribochemical reactions may lead to the formation of adsorbed layers and electric double layers (EDLs). Intermolecular forces, such as van der Waals (vdW) forces, are commonly observed between these layers. These layers allow slippage with very low shear stress and low friction.

In liquid superlubricity, the rolling/sliding conditions have been examined only little. Although superlubricity of pure glycerol was mostly explained as tribochemically induced [14, 17, 18] after running-in, the viscosity of glycerol aqueous solution is equally important, especially in rolling/sliding [19, 20].

The hygroscopicity of glycerol is also very important, which makes it possible to reduce friction when the relative humidity (RH) increases or after mixing with water [19, 21]. Depending on the amount of water, the viscous friction of glycerol and its solution can therefore be predicted independently of contact materials, which was shown by Habchi et al. [19]. This is possible by knowing the viscosity of the mixture and its dependence on the pressure and temperature. The pressure–viscosity coefficients for some mixtures with water was calculated by Shi et al. [20] from measured film thickness. However, this dependence of the lubricants is also good to be measured as Bair and Habchi [22] recommended.

The effect of the sliding-to-rolling ratio (SRR) on friction was previously investigated for glycerol solution by measurements of traction curves [19, 20, 23, 24]. The dependence of friction on the SRR was found to be almost linear. Vergne [23] named the very low friction and the absence of jump rise at low SRRs as "super low traction". The state of superlubricity and linear shape of the traction curve will be called "super low traction" in this article. Any other friction below 0.01, without respect to the shape of the traction curve, will be called "superlubricity" according to the previous definition [1].

References [25–28] have focused on polyalkylene glycol (PAG) and their aqueous solution under rolling/sliding. Yilmaz et al. [25] and Zhang et al. [29] were among a few researchers who studied the film thickness of superlubricity contact under high velocity, providing thick films. According to the mentioned literature [10–21, 23–27], there are multiple explanations for the origin of superlubricious friction in point contacts lubricated by aqueous solution of water miscible lubricants under various kinematic conditions. Therefore, the aim of the current paper is to study friction and film thickness for conditions near the transition to the mixed lubrication. Friction to the hydrodynamic fluid film friction theory and high-pressure rheology data are systematically correlated. Based on these data, it is clear what film thickness and friction is compliant with the classical theory, and what deviations are special for water solution with polyethylene glycol (PEG) under low-film conditions. It helps to improve our understanding of these lubricants under low-film conditions specific for mixed and boundary lubrication regimes. Representative samples of aqueous solution were examined for high-pressure viscosity, traction curves, and Stribeck curves in the rolling/sliding elastohydrodynamic lubrication (EHL) contact.

2 Materials and methods

Tribological experiments were performed at a laboratory temperature of 24.7±0.8 °C and an ambient humidity of 29%±2% RH. PEG with a molecular weight of 200 g/mol and a density of 1.124 g/cm^3 was purchased from Sigma-Aldrich, Inc. (Chemical Abstracts Service (CAS) No. 25322-68-3). Two volume mixtures with distilled water were prepared. The first was 18 vol% of water and named PEG200(82). The second mixture had a double amount of water, so it was labeled PEG200(64).

More solution of glycerol and water was used to achieve superlubricity and super low traction. By measuring the refractive index and comparing it with that reported in Ref. [30], the purity of the glycerol was determined to be 98 wt% (gly98). Then water solution corresponding to 40% RH [21] was prepared, i.e., 84 wt% glycerol (gly84). All lubricant mixtures are summarized in Table 1.

In order to find out the pressure–viscosity coefficient, a high-pressure viscometer (Brno University of Technology, Czech Republic) with a falling body was used, and the measured data were regressed by the McEwen model [31]. The falling body viscometer has a design inspired by Bair [32], and the used sinker was calibrated by 4 liquids (squalene, trioctyl trimellitate, di-isodecyl phthalate, and dioctyl phthalate).

Table 1 Compositions of examined lubricants.

	PEG200	Glycerol	Water
PEG200	100 vol%		
PEG200(82)	82 vol%		18 vol%
PEG200(64)	64 vol%		36 vol%
gly98		98 wt%	2 wt%
gly84		84 wt%	16 wt%

First, the pressure chamber with a lubricant sample was tempered to the selected temperature (30, 50 or 70 °C). Then the sinker fall time was measured by a linear variable displacement transducer (LVDT) sensor (multiple measurements were averaged) with pressures of 0.1, 25, 50, 100, 150, 200, 250, and 300 MPa. Subsequently, the fall time was converted to viscosity according to the equation given by Bair [32] for this type of viscometer. The obtained viscosity values were then used to determine the α^* in the McEwen model [31]. The viscosity dependence on temperature was obtained on a rotational viscometer (RotoVisco 1, Haake, Germany).

The contact bodies were a bearing ball of G3 grade from Si_3N_4 and a disc from optical glass BK7 for experiments with aqueous solution of PEG. A 100Cr6 ball and a BK7 glass disc were used for experiments with glycerol and its solution. Disc and ball were cleaned mechanically by acetone and cellulose pulp before each test. For the film thickness measurement by the optical interferometry, the glass disc was coated with a thin layer of chromium (Cr). The average roughness (S_a) of the test samples are given in Table 2.

The friction was measured by a torque sensor connected to a shaft holding ball in an optical ball-on-disc tribometer (Brno University of Technology, Czech Republic), where the film thickness was measured *in situ* by the thin film colorimetric interferometry [33]. The lubricant supply into the contact was realized by dip lubrication, as shown in Fig. 1. The parasitic torque moment of the support

Table 2 Initial S_a of samples.

	S_a (nm)
Si_3N_4 ball	9
100Cr6 ball	5
BK7 glass disc+Cr	0.7
BK7 glass disc	0.7

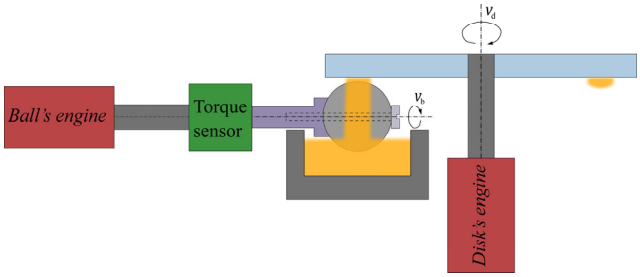

Fig. 1 Supplying lubricant from pot reservoir. Note: v_b is the speed of the ball, and v_d is the speed of the disc.

bearings was canceled out by calibration steps conducted during each experiment. A typical value of the support bearing torque corresponds to a CoF of 0.002 at 70 N of load. The linearity error of the torque sensor is CoF = 0.0003 at 70 N. The load levels were 35 and 70 N, which meant 575 and 725 MPa of contact pressure, respectively, when the silicon nitride and the optical glass were used, or 544 and 685 MPa, respectively, when the steel and the optical glass were used.

3 Results and discussion

The values of pressure–viscosity coefficients obtained by considering the McEwens model for evaluation of high-pressure viscosity measurements of two lubricants are shown in Table 3. Solution with a high amount of water, namely PEG200(82) and PEG200(64), had too small viscosity, and thus the falling body (sinker) in the viscometer was too fast to get an accurate measurement of its viscosity.

The dependence of viscosity on temperature was measured on a commercial rotational cylindrical viscometer. As the amount of water in the solution increases, the viscosity decreases significantly, as shown in Fig. 2. Therefore, it can be expected that the solution of PEG provides lower friction based on the low pressure–viscosity dependence and low viscosity at ambient pressure.

Table 3 Pressure–viscosity coefficients for two water-based lubricants.

Lubricant	α^* at 30 °C (GPa^{-1})	α^* at 50 °C (GPa^{-1})	α^* at 70 °C (GPa^{-1})
gly84	3.55	2.90	2.58
PEG200	7.84	6.52	5.76

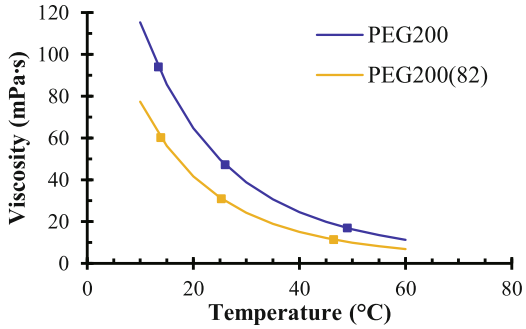

Fig. 2 Viscosity/temperature dependence for some PEG solution.

3.1 Glycerol/water solution

One of the widely studied lubricants exhibiting low friction is glycerol [1]. Figure 3 presents the results of traction curves, plotted as average shear stress calculated from the measured CoF on an average shear rate obtained from the film thickness measurement, for two concentrations of glycerol. The mean Hertzian pressure and the mean value between the central and (global) minimum film thickness were used for the conversion. Due to glycerol's hygroscopic properties, a 100 wt% concentration is not practically feasible to work under an ordinary laboratory humidity.

There is a visible slight decline from linear Newtonian viscous response in the EHL contact for almost pure glycerol at room temperature. The slope of the line for a mean speed of 50 mm/s and a concentration of 98 wt% is a little bit steeper than those for other velocity. It is probably due to the strongly hygroscopic property of high-concentration glycerol solution under the conditions of ambient humidity, as mentioned in Ref. [21]. The water solution with an amount of gly84 exhibits a lower dependency of shear stress on a shear rate. It is caused by the reduction in ambient viscosity and pressure–viscosity coefficient (Table 3). The value of 5.4 GPa^{-1} at 40 °C is reported for pure glycerol [1], while the value is 3.2 GPa^{-1} at 40 °C for gly84 sample according to the high-pressure viscometer measurement. The addition of water leads to a formation of thinner film; therefore, higher speed is necessary to obtain full separation of surfaces. It is shown in Fig. 4 that transition to mixed lubrication can be seen within the tested speed range for the solution of glycerol with water (gly84), while it is not the case of the other sample (gly98).

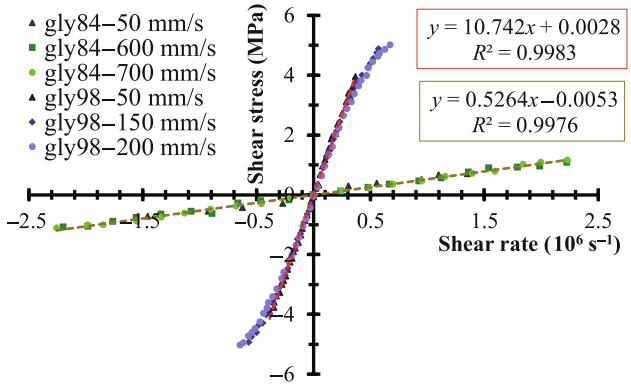

Fig. 3 Plots of average shear stress against average shear rate for EHL contact formed for glycerol (gly98) and its aqueous solution (gly84) at a load of 70 N.

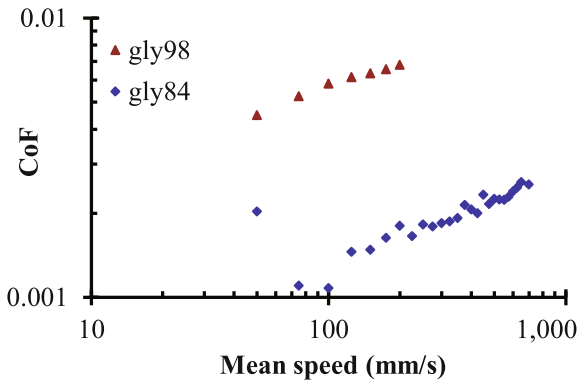

Fig. 4 Stribeck curves for glycerol (gly98) and its aqueous solution (gly84) at 50% SRR.

The diluted solution of glycerol (gly84) has effective viscosity, 526.4 mPa·s, according to the slope of the linear fit of data (Fig. 3). This value is in fair agreement with that in prediction made for mean Hertzian pressure and temperature of the experiment (23.9 °C) using the McEwens model based on the measurement in a high-pressure viscometer. It indicates that there are no tribochemical reactions important to achieve low friction under rolling/sliding conditions of the full-size EHL contact.

3.2 PEG/water solution

The first tribological measurement was realized with pure PEG200 when the contact was loaded with a normal force of 37 N. The dependence of friction on the SRR for three mean speeds is shown in Fig. 5. A linear dependence can be observed with the rising SRR, which is a sign of lubricant Newtonian responds

in an EHL contact. The SRR is defined as

$$\mathrm{SRR} = \frac{2(v_\mathrm{d} - v_\mathrm{b})}{v_\mathrm{d} + v_\mathrm{b}} \quad (1)$$

where v_b is the speed of the ball, and v_d is the speed of the disc. The linear trend has a steeper slope for higher speeds. This corresponds to that shown by Vergne [23] for pure glycerol. The points follow the linear trend already from small values of the SRR with similar magnitudes of CoF to those of pure glycerol at 40 °C [1]; thus, it can be concluded that pure PEG200 has similarly super low traction properties as glycerol.

Traction curves are replotted to the units of the average shear stress against the average shear rate by taking the measured film thickness data into consideration (Fig. 6). The slope of the linear master curve corresponds to in-contact effective viscosity of 1,217.1 mPa·s for PEG200. It is comparable to the value

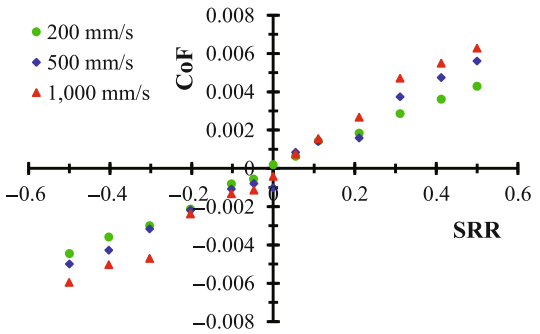

Fig. 5 Traction curves of pure PEG200 at the load of 37 N.

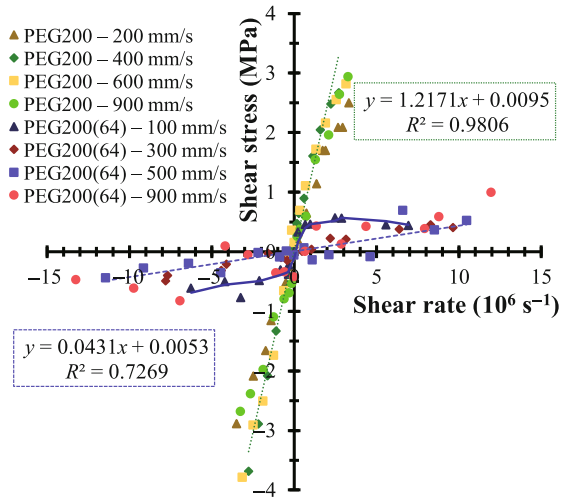

Fig. 6 Plots of contact average shear stress against average shear rate for PEG200 solution at 70 N.

obtained by a high-pressure viscometer measurement. To match the experimental values exactly with the viscosity measurement data, the effective contact temperature would be 28.2 °C, which is slightly higher than the actual ambient temperature. A small increase in temperature caused by sliding can be expected, as reported by Yilmaz et al. [25].

Alternatively, Liu et al. [34] concluded a possibility of creation of a shearing layer after a running-in phase longer than 1 h. A similar running-in phase was not necessary in our measurement of PEG200 under rolling/sliding conditions. Another observation was a decrease in lubricant viscosity with testing time due to hygroscopicity of pure polyglycols. A change in the lubricant refractive index was found after experiments especially for a pure PEG200 sample.

The water solution sample PEG200(64) (Fig. 6) has a gentler slope of shear stress with the shear rate, and the trend is linear over a wider range of shear rates than that for pure PEG200. An exception is the PEG200(64) data points for a speed of 100 mm/s. For clarity, the points are connected by a blue solid line. There can be seen a certain discrete jump in friction after flipping the orientation of the sliding. Since the following trend of shear stress on the shear rate seems to be similar with those of other PEG200(64) data for higher speeds, it indicates another source friction, which is independent of the shear rate. Friction in the boundary lubrication is usually poorly dependent on the sliding speed, and thus can be suggested that the contact is in the mixed lubrication regime. The magnitude of the friction jumps is low; therefore, it can be assumed that the contact is operated right on the threshold of the transition into mixed lubrication. Nevertheless, to correctly answer the question of mixed lubrication severity, it would be necessary to know the CoF that applies for boundary lubrication under present conditions in the contact.

An alternative explanation associated with low lubrication layer could be linked to a PEG brush layer structure adsorbed on a contact surface [34]. The combination of intermolecular forces and the interaction of PEG chains can lead to a small increase in friction after the disappearance of the fluid film. The more mobile molecules of the mixture of water and PEG200, which are present at higher velocity, are

thus probably pushed out of the contact area similar to water from an oil emulsion [35]. Subsequently, interactions of 2 adsorbed layers of PEG200 chains occur. The charged ends of these chains interact by repulsive forces. The collapse of the assumed adsorption layer could then lead to a fast increase in friction, which leads to a sudden change in shear stress. If the adsorption of PEG chains is present, no tendency for running-in of the solution was noted.

The PEG200(64) solution forms thin films between 10 and 100 nm (Fig. 7) with power trends on speed, as is obvious for the elastohydrodynamic theory [36]. However, step changes in film thickness were also observed, and they are described in the next paragraph. Despite thin films, the test surfaces were fully separated. At the moment of full separation, low friction in the contact could be achieved due to low shear resistance (viscosity) of the lubricant. The low in-contact viscosity contributes to a low pressure–viscosity coefficient. All of the results presented here support the conclusion that no tribochemical reaction plays a major role in the low friction of the water–PEG solution under present conditions used in the tests. The stability of full film separation relies on the wear behavior of the contact material. The test surfaces maintain relatively low roughness even after their surface interactions in the mixed lubrication regime (S_a = 10.1 nm for ball and 0.7–3 nm for disc—depending on a location in track).

In a detailed analysis of the data of the film thickness (Fig. 7), certain abnormality was observed for all solutions. It is a local film thickness drop in a trend that takes place below 100 nm for pure PEG200, below 70 nm for PEG200(82), and below 50 nm for PEG200(64). This experiment was repeated several times with a special focus on the transition area to eliminate the possibility of the measurement flaw. Locations of step changes were observed at the same speed and film thickness when the speed was increasing as if it was decreasing. A detailed interferogram of the film thickness is shown in Fig. 8. The speed, at which the step change takes place, is almost independent of the load. It was observed that rather than speed or load, the value of film thickness determines the transition point. A similar film thickness change was observable even for the minimum film thickness once it reaches the transition value. The power slope of the lubricant film thickness (minimum and central) was almost maintained before and after the step change. Further experiments need to be carried out in the future to fully elucidate this phenomenon.

In the past, some unexpected anomalies have been found in the film thickness of a lubricating layer for different fluids. One of the anomalies was measured by Luo et al. [37] linked to the thin film lubrication (TFL) mode. An increase in the lubricating layer thickness was found compared to a constant power slope with the decreasing speed. The explanation was the action of the adsorbed lubricant layer on the surfaces. Nevertheless, the anomaly had an opposite direction than the present deviations, as shown in Fig. 7. In other works by Zhao et al. [38] and Valtiner et al. [39], the step changes in film thickness were measured surface force apparatus (SFA) for aqueous solution with potassium chloride. Two steps were found in Ref. [38]. The first step was observed when the film thickness was about 17 nm. It was explained by vdW attractive forces. The second jump was due to the size of water molecule layer, and it was seen when the thickness was only 0.3 nm. Not so large steps were observed in Ref. [39], but smooth (few

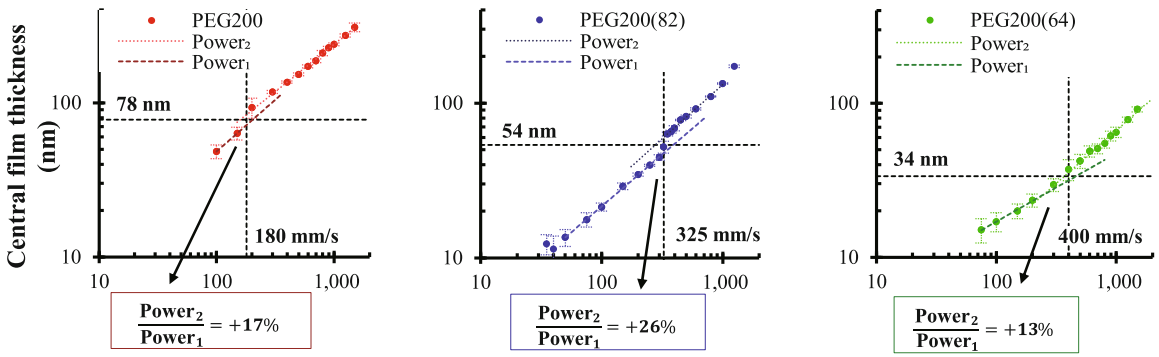

Fig. 7 Plots of central film thickness on speed for PEG solution at a load of 35 N.

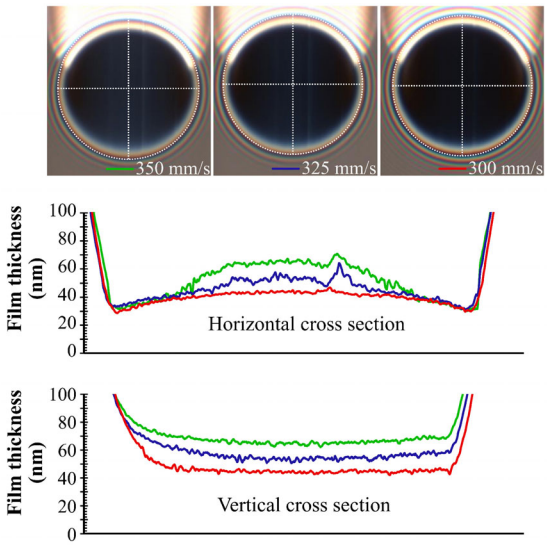

Fig. 8 Interferograms of contact lubricated with PEG200(82) during a step change in film thickness at a load of 35 N.

angstroms) as well as rough (root mean square (RMS) 17 Å) surfaces were used to investigate the effect of roughness. It was concluded that the extended Derjaguin–Landau–Verwey–Overbeek (DLVO) theory could describe jumps with consideration of surface roughness, hydration forces, attractive (vdW), and repulsive forces (EDL). It is possible that these small interaction forces and film layers are involved in the step changes in the thickness of the lubricating film (Fig. 7).

The influence of free and bound water molecules in the PAG solution on the magnitude of friction was previously discussed by Wang et al. [40] and Liu et al. [34]. Both studies consider that adsorbed lubricant layers are formed on the surfaces. Between these layers, there can be hydrated PAG molecules, free water molecules, or a combination thereof. The step change in Fig. 7 would then probably be a consequence of the reduction of the adsorbed layers and the change in the orientation of the PAG chains. But it is difficult to imagine not only the change in the thickness of the lubricating film but also the obvious change in viscosity before and after the jump, which would be caused in this way.

Another possibility could be a change in the orientation of the PEG200 molecule with bound water. In its normal state, the molecule in solution is probably in the "trans–trans–gauche" conformation [41], and despite its short length (approx. 4 ethylene glycol monomers), its nonlinear arrangement can be assumed. Reducing the thickness of the lubricant can mean not only the straightening of the PEG200 chains themselves but also a change in their conformation to "all trans". A change in the behavior of lubricant molecules can then be the reason for a change in viscosity, which can be observed after the jump in Fig. 7.

It is appropriate to discuss the jumps from the point of view of classical tribology. If the lambda parameters (λ) were calculated as Vergne [23] did (disc RMS = 0.6 nm and ball RMS = 16.9 nm), the values would be for the jump region for PEG200 from 3.7 to 5.5. It means that the surfaces are fully separated. For PEG200(82), the calculated values are 2.6 to 3.7, and thus there may be occasional local contacts. For PEG200(64), the lambda values are 1.8 to 2.2, and the separation of surfaces is even lower. The possibility of transition to mixed lubrication is not supported by data of friction (Fig. 6) for speeds of the film steps in Fig. 7. The surface of the glass could be considered almost smooth, and the roughness on the ball surface had the shape of dents elastically deformed inside the EHL contact; therefore, the contact was fully separated, which corresponds to optical observation, and the film thickness jumps are not caused by contacts of asperities.

Figure 8 shows the interferograms of the contact and film thickness profiles for three speeds around step change for PEG200(82). In the horizontal cross section profile, the area of the minimum film thickness is hardly affected, while a significant increase of the film thickness takes place close to the contact centerline. It could be said that there is full surface separation for both states before and after the step change in central film thickness. Thus, the lubrication regime did not change.

Another important change can be seen in the vertical profiles (Fig. 8). The film profile for speed before the step change (350 mm/s) exhibits much more curved shape in the central EHL zone compared to the profile after the step change (300 mm/s). The curve shape of the film thickness in the central zone is related to lubricant compressibility or due to pressure-induced flows (Poiseuille flow). The later effect causes the decrease of the monotonic film in contact entrainment direction due to its natural effect on speed profile. Because it cannot be seen in the present profiles, one

can conclude that there is an abrupt change of lubricant compressibility. It can be explained by the change of the relative water concentration or PAG chain conformation [41] after the step film change. It leads to an increase in effective viscosity connected with thicker film formation according to the EHL theory. During the transition, it presents local inhomogeneity, which influences the contact center. For slightly higher speeds, i.e., thicker films, the contact edges, i.e., the minimum film thickness, remain affected. The behavior is all over the contact inlet. A further increase in speed already leads to the shape of film profiles once again according to a classical EHL theory.

4 Conclusions

Water-based lubricants, namely glycerol, PEG, and their water solution, were studied. Experiments for film thickness, traction curves, and friction-speed curves were conducted in an optical tribometer for various operating conditions to study the lubrication regime and origins of low friction.

It was found that the viscosity of the fluids and full film separation of surfaces are the principal reasons for the occurrence of the superlubricity in the macroscale contacts under studied operating conditions. Although vdW or EDL repulsive forces were expected to play a role in surface separation, no significant signs of those were observed in present experiments. In present observations, formation of the EHL film can be explained by a classical EHL theory, and friction originates from the viscous behavior of fluid film, where full separation of surfaces is important. Studied fluids exhibit the superlubricity due to their low ambient viscosity and low pressure–viscosity coefficients. Added water reduces viscosity and pressure–viscosity dependence; therefore, the mean shear stress and friction inside an EHL contact are low. Additional contribution to the friction can be affected by intermolecular and surface forces, especially near to transition between mixed and elastohydrodynamic regimes. However, the interactions are not large enough to be reliably demonstrated in friction measurements under studied conditions.

An exception of a film thickness anomaly was observed for the PEG200 and its solution close to conditions of transition to mixed lubrication. With the decreasing speed, there is a step change to a lower film thickness with maintaining the power slope, which is a sign of step viscosity change. Several mechanisms and explanations have been discussed in the paper. The most probable is a change conformation/concentration of PEG chains and water molecules in the contact inlet connected with the step change in effective viscosity.

Acknowledgements

The research was supported by the Czech Science Foundation (No. 21-28352S).

Declaration of competing interest

The authors have no competing interests to declare that are relevant to the content of this article.

References

[1] Erdemir A, Martin J M. *Superlubricity*. Amsterdam, the Netherlands: Elsevier Amsterdam, 2007.

[2] Kano M. Super low friction of DLC applied to engine cam follower lubricated with ester-containing oil. *Tribol Int* **39**(12): 1682–1685 (2006)

[3] De Barros Bouchet M I, Kano M. Superlubricity of diamond/glycerol technology applied to automotive gasoline engines. In: *Superlubricity*. Erdemir A, Martin J M, Eds. Amsterdam, the Netherlands: Elsevier Amsterdam, 2007: 471–492.

[4] Baykara M Z, Vazirisereshk M R, Martini A. Emerging superlubricity: A review of the state of the art and perspectives on future research. *Appl Phys Rev* **5**(4): 041102 (2018)

[5] Li J J, Luo J B. Advancements in superlubricity. *Sci China Technol Sc* **56**(12): 2877–2887 (2013)

[6] Mutyala K C, Doll G L, Wen J G, Sumant A V. Superlubricity in rolling/sliding contacts. *Appl Phys Lett* **115**(10): 103103 (2019)

[7] Li J J, Ge X Y, Luo J B. Random occurrence of macroscale superlubricity of graphite enabled by tribo-transfer of multilayer graphene nanoflakes. *Carbon* **138**: 154–160 (2018)

[8] Ge X Y, Li J J, Luo J B. Macroscale superlubricity achieved with various liquid molecules: A review. *Front Mech Eng* **5**: 2 (2019)

[9] Li J J, Zhang C H, Deng M M, Luo J B. Investigation of the difference in liquid superlubricity between water- and oil-based lubricants. *RSC Adv* **5**(78): 63827–63833 (2015)

[10] Fang Y F, Ma L R, Luo J B. Modelling for water-based liquid lubrication with ultra-low friction coefficient in rough surface point contact. *Tribol Int* **141**: 105901 (2020)

[11] Xu J G, Kato K. Formation of tribochemical layer of ceramics sliding in water and its role for low friction. *Wear* **245**(1–2): 61–75 (2000)

[12] Raviv U, Giasson S, Kampf N, Gohy J F, Jérôme R, Klein J. Lubrication by charged polymers. *Nature* **425**(6954): 163–165 (2003)

[13] Li J J, Zhang C H, Ma L R, Liu Y H, Luo J B. Superlubricity achieved with mixtures of acids and glycerol. *Langmuir* **29**(1): 271–275 (2013)

[14] Long Y, de Barros Bouchet M I, Lubrecht T, Onodera T, Martin J M. Superlubricity of glycerol by self-sustained chemical polishing. *Sci Rep* **9**: 6286 (2019)

[15] Ge X Y, Halmans T, Li J J, Luo J B. Molecular behaviors in thin film lubrication—Part three: Superlubricity attained by polar and nonpolar molecules. *Friction* **7**(6): 625–636 (2019)

[16] Ge X Y, Li J J, Zhang C H, Luo J B. Liquid superlubricity of polyethylene glycol aqueous solution achieved with boric acid additive. *Langmuir* **34**(12): 3578–3587 (2018)

[17] Deng M M, Li J J, Zhang C H, Ren J, Zhou N N, Luo J B. Investigation of running-in process in water-based lubrication aimed at achieving super-low friction. *Tribol Int* **102**: 257–264 (2016)

[18] Matta C, Joly-Pottuz L, de Barros Bouchet M I, Martin J M, Kano M, Zhang Q, Goddard W A. Superlubricity and tribochemistry of polyhydric alcohols. *Phys Rev B* **78**(8): 085436 (2008)

[19] Habchi W, Matta C, Joly-Pottuz L, Barros M I, Martin J M, Vergne P. Full film, boundary lubrication and tribochemistry in steel circular contacts lubricated with glycerol. *Tribol Lett* **42**(3): 351–358 (2011)

[20] Shi Y J, Minami I, Grahn M, Björling M, Larsson R. Boundary and elastohydrodynamic lubrication studies of glycerol aqueous solutions as green lubricants. *Tribol Int* **69**: 39–45 (2014)

[21] Chen Z, Liu Y H, Zhang S H, Luo J B. Controllable superlubricity of glycerol solution via environment humidity. *Langmuir* **29**(38): 11924–11930 (2013)

[22] Bair S, Habchi W. Your EHD rig may not be as elastohydrodynamic as you think. *J Tribol* **143**(8): 081601 (2021)

[23] Vergne P. Super low traction under EHD & mixed lubrication regimes. In: *Superlubricity*. Erdemir A, Martin J M, Eds. Amsterdam, the Netherlands: Elsevier Amsterdam, 2007: 427–443.

[24] Björling M, Shi Y J. DLC and glycerol: Superlubricity in rolling/sliding elastohydrodynamic lubrication. *Tribol Lett* **67**(1): 23 (2019)

[25] Yilmaz M, Mirza M, Lohner T, Stahl K. Superlubricity in EHL contacts with water-containing gear fluids. *Lubricants* **7**(5): 46 (2019)

[26] Kamga L S, Oehler M, Sauer B. Characterization of the viscoelastic behaviour of gears oils by EHL simulation. In: Proceedings of the 14th World Congress on Computational Mechanics (WCCM), Paris, France, 2021: 1–8.

[27] Gangopadhyay A, Liu Z, Simko S J, Peczonczyk S L, Cuthbert J B, Hock E D, Erdemir A, Ramirez G. Friction and wear reduction mechanism of polyalkylene glycol-based engine oils. *Tribol Trans* **61**(4): 621–631 (2018)

[28] Zhang J, Tan A, Spikes H. Effect of base oil structure on elastohydrodynamic friction. *Tribol Lett* **65**(1): 13 (2016)

[29] Zhang C H, Zhao Y C, Björling M, Wang Y, Luo J B, Prakash B. EHL properties of polyalkylene glycols and their aqueous solutions. *Tribol Lett* **45**(3): 379–385 (2012)

[30] Glycerine Producers' Association. *Physical Properties of Glycerine and Its Solutions*. New York: Glycerine Producers' Association, 1963.

[31] Bair S. *High Pressure Rheology for Quantitative Elastohydrodynamics*, 2nd edn. Amsterdam, the Netherlands: Elsevier Amsterdam, 2019.

[32] Bair S. A routine high-pressure viscometer for accurate measurements to 1 GPa. *Tribol Trans* **47**(3): 356–360 (2004)

[33] Hartl M, Křupka I, Liška M. Elastohydrodynamic film thickness mapping by computer differential colorimetry. *Tribol Trans* **42**(2): 361–368 (1999)
[34] Liu W R, Wang H D, Liu Y H, Li J J, Erdemir A, Luo J B. Mechanism of superlubricity conversion with polyalkylene glycol aqueous solutions. *Langmuir* **35**(36): 11784–11790 (2019)
[35] Liu H C, Pape F, Zhao Y, Ellersiek L, Denkena B, Poll G. On the elastohydrodynamic film-forming properties of metalworking fluids and oil-in-water emulsions. *Tribol Lett* **71**(1): 10 (2023)
[36] Hamrock B J, Dowson D. Isothermal elastohydrodynamic lubrication of point contacts: Part I—Theoretical formulation. *J Lubrication Tech* **98**(2): 223–228 (1976)
[37] Luo J B, Wen S Z, Huang P. Thin film lubrication. Part I. Study on the transition between EHL and thin film lubrication using a relative optical interference intensity technique. *Wear* **194**(1–2): 107–115 (1996)
[38] Zhao G T, Tan Q Y, Xiang L, Cai D, Zeng H B, Yi H, Ni Z H, Chen Y F. Structure and properties of water film adsorbed on mica surfaces. *J Chem Phys* **143**(10): 104705 (2015)
[39] Valtiner M, Banquy X, Kristiansen K, Greene G W, Israelachvili J N. The electrochemical surface forces apparatus: The effect of surface roughness, electrostatic surface potentials, and anodic oxide growth on interaction forces, and friction between dissimilar surfaces in aqueous solutions. *Langmuir* **28**(36): 13080–13093 (2012)
[40] Wang H D, Liu Y H, Li J J, Luo J B. Investigation of superlubricity achieved by polyalkylene glycol aqueous solutions. *Adv Mater Interfaces* **3**(19): 1600531 (2016)
[41] Oesterhelt F, Rief M, Gaub H E. Single molecule force spectroscopy by AFM indicates helical structure of poly(ethylene-glycol) in water. *New J Phys* **1**: 6 (1999)

Tomáš POLÁČEK. He received his bachelor's and M.S. degrees in mechanical engineering from Brno University of Technology, Czech Republic, in 2019 and 2021, respectively. Now he is a Ph.D. student in Institute of Machine and Industrial Design, Faculty of Mechanical Engineering, Brno University of Technology, Czech Republic. His research interests include mixed and elastohydrodynamic friction and superlubricity.

Petr ŠPERKA. He received his M.S. and Ph.D. degrees in mechanical engineering from Brno University of Technology, Czech Republic, in 2007 and 2011, respectively. His current position is an assistant professor and head of Elastohydrodynamic Lubrication Section at Tribology Group, Institute of Machine and Industrial Design, Faculty of Mechanical Engineering, Brno University of Technology, Czech Republic. His research areas cover the boundary, mixed and elastohydrodynamic lubrication, roughness effect, and lubricant rheology.

Ivan KŘUPKA. He received his M.S. and Ph.D. degrees in mechanical engineering from Brno University of Technology, Czech Republic, in 1990 and 1997, respectively. His current position is a professor and head of Tribology Group, Institute of Machine and Industrial Design, Faculty of Mechanical Engineering, Brno University of Technology, Czech Republic. His research areas cover the mixed and elastohydrodynamic lubrication, surface texturing effect, and lubricant rheology.